Effect of Thermal Radiation during Annealing on Self-organization of Thin Silver Films

Victor Ovchinnikov
Department of Aalto Nanofab
School of Electrical Engineering, Aalto University
Espoo, Finland
e-mail: Victor.Ovchinnikov@aalto.fi

***Abstract*—Fabrication method of self-organized silver nanostructures by annealing of thin films is studied. The method has poor reproducibility and generates different shapes and sizes of nanostructures for identical conditions, but in different furnaces. To clarify the source of instability, the self-organized nanostructures were prepared by annealing of silver films with different strength of thermal radiation. The results demonstrate dependence of morphology and reflectance spectra of the samples on power of thermal radiation. Numerical simulations of heating conditions were performed and confirmed effect of thermal radiation on melting of silver nanostructures. The obtained results can be used to control self-organization of silver nanostructures and to improve reproducibility of the fabrication processes.**

Keywords-self-assembling; silver nanostructure; random array; annealing

I. INTRODUCTION

Metal nanostructures are widely used in different applications ranging from plasmonics [1] and nanopatterning [2,3] to chemical catalyst [4] and metamaterials [5]. The most attractive are silver and gold nanostructures, because they possess plasmon resonances in visible range of wavelength and are used in biosensors [6], surface enhanced Raman spectroscopy (SERS) [2], near field optics [7], etc. Despite of this, industrial application of regular or periodic metal nanostructure arrays is hindered by high cost and complexity of their fabrication. In view of this, significant attention is devoted to study of random or irregular arrays of metal nanostructures and their applications instead of regular arrays. In random arrays, nanostructure shape and space periodicity are varied in the limited range. As a result, random nanostructure arrays still possess resonance features, similar to periodic arrays, but they are not so sharp and strong. It is still suitable for many applications and irregular arrays are widely used in SERS substrate [2] and thin film solar cells [8,9]. Most attractive are random arrays in which one or more parameters are fixed and are not varied, e.g., thickness of all structures is the same or all asymmetric structures are oriented in the same direction or shape of all nanoislands is spherical.

One of the easiest and oldest methods to produce irregular array of metal nanoislands is physical vapor deposition of ultra thin metal film [10-12]. The method works well for film thickness less than 5 nm, when as deposited film consists of isolated nanoislands. At higher thicknesses, when deposited film is lace-like, self-organization of nanoislands can be stimulated by annealing [13,14]. Depending on film material and thickness, annealing cab be done at different temperatures (200 – 800 C), in different ambient (vacuum or gas) and in the time interval from 1 second to several hours. In the resulting nanostructure array, nanoisland size and separation between nanoislands are usually variable, but shape is similar for most of structures on a substrate, e.g., array of ellipsoids or array of peanut-shaped structures [15].

Many papers are devoted to fabrication and study of metal nanospheres, due to potential applications in plasmonics and nanotechonology. The results reported demonstrate broad range of shapes and sizes of nanospheroids for similar fabrication conditions (sample size, film thickness and annealing temperature) [13,14,16]. At the same time, all studies have common features: 1) the diameter of spheres is less than 30 nm or film thickness is less than 8 nm; 2) the sample size is less than 2 x 2 cm^2; 3) there are no details of annealing process and especially no information about relative strength of heating modes (conduction, convection and radiation). Strength of heating modes depends on furnace design, sample holder, position of sample inside of heating volume etc. Any break out of above mentioned limits leads to nanoislands of irregular (non spherical) shape. Due to this, successful reproducing of reported results in other furnace is problematic. In first turn, it concerns preparation of silver and gold nanostructures, which are often formed by annealing.

In this paper, we report on the silver film annealing in controllable conditions with different strength of thermal radiation. At the same time numerical simulations are performed to define variations of heat fluxes through the sample surface. These simulations are compared with corresponding experimental results, to find heating conditions for reproducible formation of silver nanosphere arrays.

The paper is organized as follows. In the subsequent section II, details of sample preparation and measurement procedures are presented. In the section III, the results of work are demonstrated by SEM images and reflectance spectra of the nanostructure arrays and also by heat transfer simulations. The optimal conditions of silver film annealing are discussed in Section IV.

 ISBN: 978-1-61208-303-2

II. EXPERIMENTAL

We have studied 12 nm thick silver films, deposited by electron beam evaporation at rate 0.5 nm/s. As a substrate were used pieces of 4" silicon wafer with 10 nm layer of thermal oxide. Annealing was done in diffusion furnace in nitrogen ambient. To measure temperature of the samples, a copper plate with a hole for thermocouple was used as a holder. The sample had good thermal contact with the holder which was located on the quartz boat during experiment. The furnace tube was opened from one edge to provide manual loading and unloading of the samples at temperature of annealing. The tube temperature was measured by thermocouple and stabilized at 400 C.

Two series of samples were prepared to study effect of thermal radiation on silver self-organization. In the first series the intensity of thermal radiation was controlled by the shield above the sample, in the second series the samples were heated on the holder in loading zone of the furnace. In this case there was only radiation cooling of the sample, because holder was hotter than furnace tube walls.

In the first series (tube annealing), the holder was preheated to 130 C in the central part of the furnace tube and moved to loading zone of the tube. After sample loading the holder was moved in the central zone of the tube. The holder with sample was heated up during 11 minutes and moved out from the central zone to load zone and the sample was taken out. The first sample was opened to heat radiation from the quartz tube walls, because it was not covered by anything. Another two samples were covered by shield (thin plate) to reduce heat radiation. As a material of shield were used silicon and stainless steel (UNS 304) plates with thicknesses 0.7 mm and 1 mm, respectively. The shield had sizes 75 x 85 mm^2 and supported above copper holder on the height 2.5 mm by ceramic posts. The samples were labeled corresponding to tube annealing and protective plate as T, T-Si and T-304 for uncovered, silicon covered and steel covered samples, respectively.

In the second series (hot plate annealing), the holder was heated to target temperature in the central part of the furnace and moved out for sample loading. The sample was loaded on the hot holder and left in the load zone of the furnace for 1 minute. During this time the sample and the copper holder were brought to heat equilibrium. After that the sample was taken out. The samples were labeled corresponding to hot plate annealing and temperature as HP165, HP220, HP295 for annealing at 165 C, 220 C and 295 C, respectively.

The metal films were deposited in e-beam evaporation system IM-9912 (Instrumentti Mattila Oy) at base pressure of 2×10^{-7} Torr and at room temperature of the substrate.

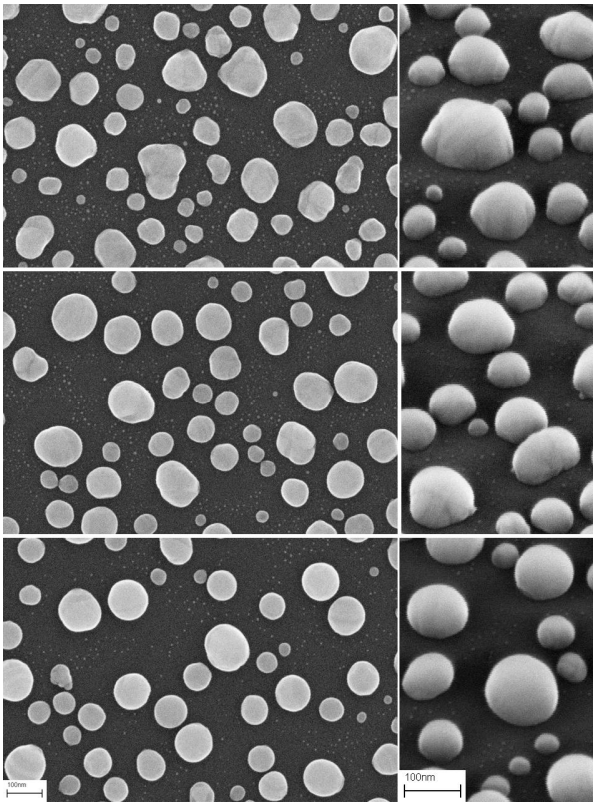

Figure 1. Plan and tilted 45° SEM images of tube annealed samples. From top to bottom T, T-Si and T-304, unprotected and protected by silicon and steel, respectively.Scale bar is 100 nm.

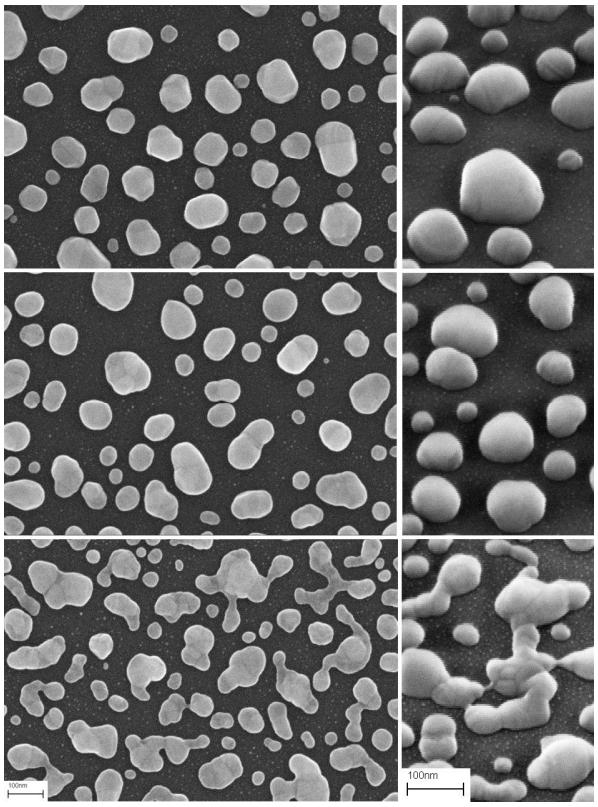

Figure 2. Plan and tilted 45° SEM images of hot plate annealed samples. From top to bottom HP295, HP220 and HP165, annealed at 295 C, 220 C and 165 C, respectively. Scale bar is 100 nm.

 ISBN: 978-1-61208-303-2

Annealing was done in the diffusion furnace THERMCO Mini Brute MB-71. Plan view and tilted at 45^0 SEM images of the samples were observed with Zeiss Supra 40 field emission scanning electron microscope. Reflectance measurements at normal incidence were carried out using FilmTek 2000M reflectometer in the spectral range from 380 to 890 nm.

III. RESULTS

Fig. 1 shows plan view and tilted SEM images of the tube annealed samples. The samples have close values of areal density and nanostructure sizes, but shape of nanoislands depends on annealing conditions. The unprotected sample T demonstrates most irregular islands with straight flats on some of them. The sample with silicon shield T-Si has roundish nanostructures with large shape deviation and the sample with steel shield T-304 shows spherical nanoislands with bi-modal distribution of diameters. It is visible on the tilted images, that nanospheres of the sample T-304 touch substrate at small contact area. In case of samples T and T-Si this contact area is larger and height of nanostructures is less than for sample T-304.

Fig. 2 shows plan view and tilted SEM images of the hot plate annealed samples. In this series shape variations are more significant. It is observed lace like structures for low temperature annealed sample HP165, irregular shapes with rounded corners for the sample HP220 and irregular shapes with flats for high temperature annealed sample HP295. The tilted images demonstrate lowest thickness of nanostructures at the sample HP165 and highest thickness of nanostructures at the sample HP295. The largest contact area with substrate has sample HP220. Tube annealed sample T and hot plate annealed sample HP295 possess flats and look similar. Samples HP220 and T-Si are also similar. The sample HP165 from the second series has no analogue in the first series of samples.

It is need to note that samples have different colours of the surface. The samples T, T-Si and HP295 are green, the sample T-304 is blue, the sample HP220 is grey-blue and the sample HP165 is grey. Colour difference is explained by different reflection spectra which are connected with plasmonic properties of the structures. Fig. 3a demonstrates reflection spectra of the tube annealed samples. According to surface colour, the samples T, T-Si have similar reflection spectra with main peak at wavelength 490 nm and trough at 750 nm. The sample T-304 has main peak at shorter wavelength 450 nm and trough at 640 nm. The coincidence of spectra for samples T and T-Si is unexpected, because they have different SEM images. On the other hand, samples T-Si and T-304 have similar SEM images, but different reflection spectra. Dotted line shows spectrum of the as deposited silver film, i.e., spectrum of the samples before annealing. Fig. 3b demonstrates reflection spectra of the hot plate annealed samples. The low temperature sample HP165 has spectrum similar to as deposited silver film. The sample HP220 has spectrum similar to T-304, but with lower height of peak and wider trough. The spectrum of sample HP295 is close to the spectrum of sample T, only it has wider and weaker peaks.

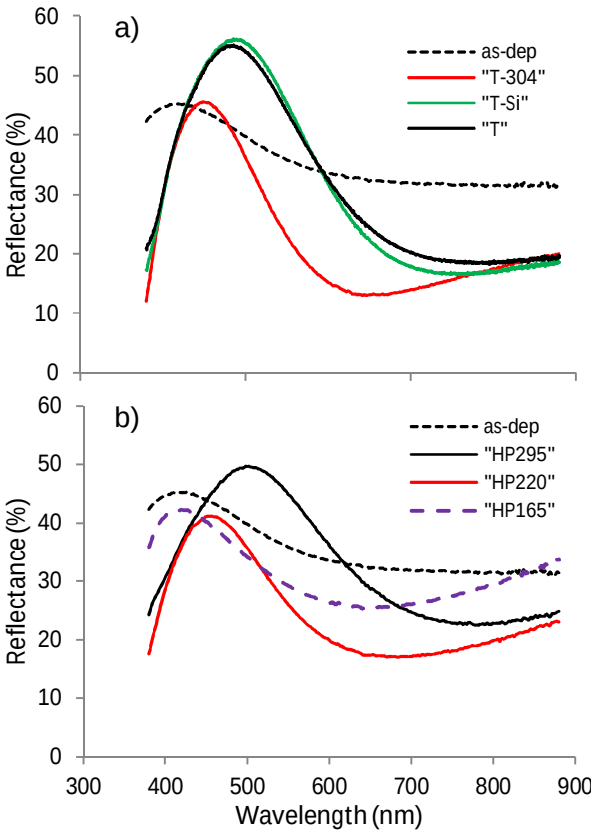

Figure 3. Reflection spectra of tube annealed (top) and hot plate annealed (bottom) samples.

The simulations were done with the help of software COMSOL Multiphysics 3.5a. It was used general heat transfer model for annealing in nitrogen ambient. The effect of heat convection was simulated for laminar nitrogen flow with velocity 0.03 m/s by means of heat transfer coefficients from the COMSOL library. The simulations were verified by

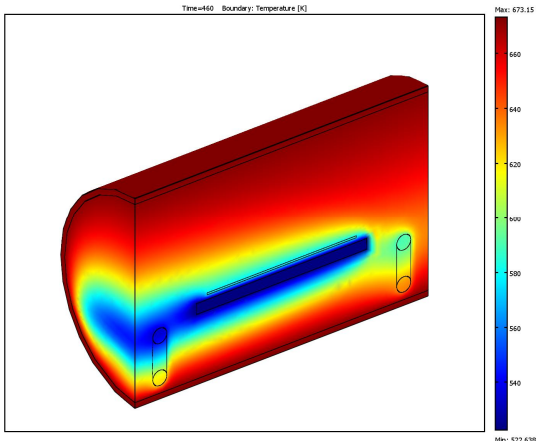

Figure 4. Calculated temperature distribution around quartz boat and copper holder during annealing of steel protected sample T-304. The copper holder has the lowest temperature.

 ISBN: 978-1-61208-303-2

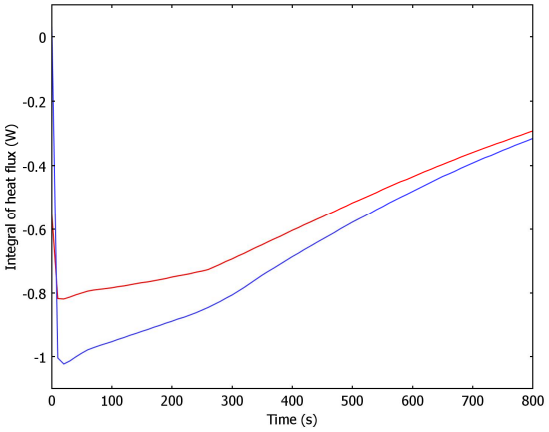

Figure 5. Calculated conductive heat flux (blue) and radiative flux (red) through the upper surface of the copper holder during annealing of uncoverd sample T.

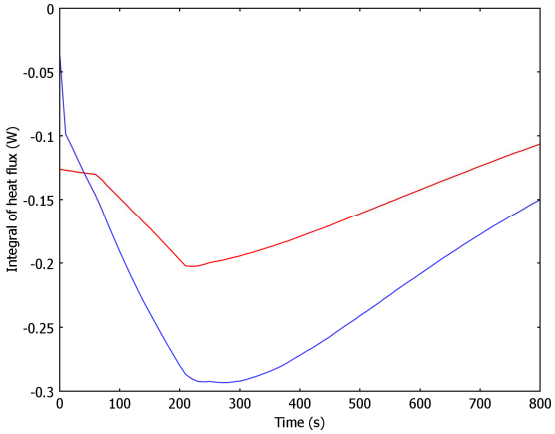

Figure 7. Calculated conductive heat flux (blue) and radiative flux (red) through the upper surface of the copper holder during annealing of sample T-304 with steel shield.

matching of calculated and measured heating curves of the copper holder (not shown). Fig. 4 demonstrates example of temperature distribution in the furnace with steel covered sample T-304. The distribution is given for the holder temperature 250 C, which is close (see below) to the melting point of silver nanostructres. The heat source and the heat sink are furnace walls and the copper holder, respectively. The vertical objects in the left-bottom and right-bottoms corners of the Fig.4 are cross-sections of the quartz boat.

Fig. 5 demonstrates variations of heat fluxes for the uncovered sample T during annealing. The flux is calculated over upper surface of the sample and has positive sign in direction of normal to the surface, i.e., outside of the sample. In this case, the conductive heat flux and the radiative flux have comparable values and decreased during heating of the sample. Fig. 6 shows evolution of holder and steel shield temperatures during annealing of the sample T-304. In the beginning, the shield is heated faster, but in stationary mode

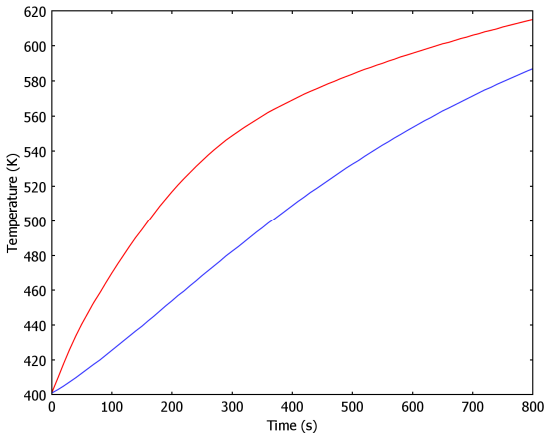

Figure 6. Calculated temperatures of the copper holder (blue) and steel shield (red) during annealing of steel protected sample T-304.

the temperatures of the shield and holder are close to each other. The maximum difference in the holder and shield temperatures (overheating) happens after 250 s of heating. Fig. 7 illustrates effect of shielding of infrared radiation by steel plate. The simulations confirm intuitive feeling that metal shield should decrease the radiation heating of the sample. Indeed, radiation flux of uncovered sample is four times more intensive than for protected one (Fig.5 and Fig.7), when samples have temperature 250 C. The radiation still exists in the shielded sample due to overheating of the shield relatively sample (55 C for the sample T-304), which in turn irradiates the sample. The most attractive in the annealing of the protected sample is three times less conductive flux in comparison with uncovered sample (Fig.5 and Fig.7). It is very important in preventing quenching of melted silver droplets (see below).

IV. DISCUSSION

Melting of silver nanostructures at low temperature annealing has been reported in several studies [14,17,18]. In case of liquid silver, the spherical shape of nanoislands for sample T-304, can be explained by droplet formation on non-wettable surface due to cohesive forces. On other hand, the results of hot plate annealing demonstrate existing of temperature point at which shape of nanoislands is changed. With the help of additional hot plate samples it was found that the point of shape transformation is close to 245 C. The result of annealing at low temperature looks like nanostructures of sample HP220, the annealing at high temperature provides nanostructures similar to sample HP295. The close results were obtained in several studies reported about melting temperature of silver nanostructures in the interval of 250-300 C [17,18]. Therefore, we believe that during our experiments the silver films heated above 245 C were melted, e.g., in samples with flats HP395 and T.

Silver properties modification caused by melting leads to changing of reflection spectra after annealing. It has been already mentioned that areal density and average size of

nanoislands are close to each other in studied samples. However, redshift of dipolar resonance in melted samples is relatively large and cannot be only explained by changing of island geometry. Resonance wavelength shift can be provided by changing of dielectric environment or dielectric function of silver in melted samples. Due to identical environment in the studies samples, it can be concluded that spectrum variations are connected with dielectric function of silver. Moreover, from spectral peak and trough broadening follows that not only real, but imaginary part of silver dielectric function was changed. One of the possible explanations is increased defect concentration in melted samples, how it was reported earlier [19].

It cost to note that additionally to bulk melting (discussed above) in nanostructures exists also surface melting or pre-melting. Pre-melting happens at lower temperature [17] and is responsible for shape variation between samples HP165 and HP220. But surface melting is not connected with increasing of defect concentration in resulting nanoislands (Fig. 3b).

Reflection spectra (Fig.3) demonstrate plasmon properties of silver nanostructres. The troughs in the range 650 – 750 nm correspond to dipole plasmon resonance and peaks at 450 – 500 nm correspond to quadrupole resonance. The different appearance in the reflection is connected with different radiation patterns of dipole and quadrupole [13]. These resonances are valid for annealed samples. Non annealed samples possess very broad range of infrared radiation (see spectrum of as deposited sample). During annealing silver temperature is higher than temperature of the substrate due additional radiation heating [20-22]. After melting liquid silver nanoislands are divided in smaller ones due to Rayleigh instability [14]. Geometry change causes blueshift of plasmon resonance, observed in the measured spectra and interruption of infrared heating, because radiation with new resonance wavelength does not exist. The cold substrate (Fig. 4) cools down silver nanostructures and causes their solidification. Our estimation for 100 nm sphere gives transition time to thermal equilibration with substrate in the range of 10^{-8} s. So fast quenching happens without proper crystallization and generates defects in silver lattice.

In case of tube annealing of protected samples melting happens at higher holder temperature. Depending on conductive and radiative heat fluxes the melted silver is cooled with much lower rate (sample T-Si) or does not solidify at all (sample T-304). For the hot plate annealing there is also quenching mechanism, despite of absence of radiation. Silver nanostructure is heated by substrate and cooled by nitrogen. In other words, there is heat flow from the substrate to ambient through nanostructure. This heat flow creates temperature drop on the interfacial thermal resistance between substrate and silver droplet, what in turn leads to decreasing of silver temperature and quenching.

V. CONCLUSIONS

We have demonstrated the effect of thermal radiation on furnace annealing of thin silver films. Due to plasmon resonance in infrared, the radiation heating of silver films can be very strong and provides overheating of the silver nanostructures relatively substrate. This overheating is self-limited owing to size dependence of resonance wavelength. After melting and fragmentation of silver nanostructures to smaller nanoislands, plasmon resonance is shifted to visible range and does not support any more heating of silver nanoislands. As a result, they are quenched to solid state with irregular shape and high defect concentration. The minimization of radiation heating supports nanostructures in liquid state after melting, providing spherical shape of nanoislands after solidification. This opens new approaches to fabrication of self-assembled silver nanostructures.

ACKNOWLEDGMENT

This research was undertaken at the Micronova Nanofabrication Centre, supported by Aalto University.

REFERENCES

[1] M. A. Garcia, “Surface plasmons in metallic nanoparticles: fundamentals and applications”, J. Phys. D: Appl. Phys., vol. 44, 2011, p. 283001, (20pp.).

[2] A. Shevchenko, V. Ovchinnikov, and A. Shevchenko, ”Large-area nanostructured substrates for surface enhanced Raman spectroscopy”, Appl. Phys. Lett., vol. 100, 2012, p. 171913 (4pp.).

[3] V. Ovchinnikov and A. Shevchenko, “Self-organization-based fabrication of stable noble-metal nanostructures on large-area dielectric substrates”, Journal of Chemistry, vol. 2013, 2013, Article ID 158431, 10pp., http://dx.doi.org/10.1155/2013/158431.

[4] Y. F. Guan, A. V. Melechko, A. J. Pedraza, M. L. Simpson, and P. D. Rack, “Non-lithographic organization of nickel catalyst for carbon nanofiber synthesis on laser-induced periodic surface structures,” Nanotechnology, vol. 18, 2007, pp. 335306 – 335312.

[5] E. Cortes, L. Mochán, B. S. Mendoza, and G. P. Ortiz, “Optical properties of nanostructured metamaterials”, Phys. Status Solidi B, vol. 247, 2010, pp. 2102 – 2107.

[6] J. N. Anker et al., “Biosensing with plasmonic nanosensors”, Nature Materials, vol. 7, 2008, pp. 442 – 453.

[7] X. Zhang and Z. Liu, “Superlenses to overcome the diffraction limit”, Nature Materials, vol. 7, 2008, pp. 435 – 441.

[8] X. Sheng et al., “Design and non-lithographic fabrication of light trapping structures for thin film silicon solar cells”, Adv. Mater. vol. 23, 2011, pp. 843 – 847.

[9] C. Eminian, F.-J. Haug, O. Cubero, X. Niquille, and C. Ballif, “Photocurrent enhancement in thin film amorphous silicon solar cells with silver nanoparticles”, Progress in Photovoltaics: Research and Applications, vol. 19, 2011, pp. 260 – 265.

[10] J. Maa and T. E. Hutchinson, “Early growth of thin films deposited by ion beam sputtering”, J. Vac. Sci. Technol., vol.14, 1977, pp. 116-121.

[11] M. Gnanavel, D.B. Mohan, and C.S. Sunandana, “Optics of quasi-particle phase transitions in nanostructured Ag thin films”, Thin Solid Films, vol. 517, 2008, pp. 1058 – 1062.

[12] G. Xu, M. Tazawa, P. Jin, and S. Nakao, “Sufrace plasmon resonance of sputtered Ag films: substrate and mass thickness denepndence”, Appl. Phys. A, vol. 80, 2005, pp. 1535-1540.

[13] J.W. Little, T.A. Callcott and T.L. Ferrell, “Sufrace-plasmon radiation from ellipsoidal silver spheroids”, Phys. Rev. B, vol. 29, 1984, pp.1606-1615.

 ISBN: 978-1-61208-303-2

[14] S.R. Bhattacharyya et al., “Growth and melting of silicon supported silver nanocluster films”, J. Phys. D: Appl. Phys., vol. 42, 2009, p. 035306 (9pp.).

[15] S. Karim et al., “Morphological evolution of Au nanowires controlled by Rayleigh instability”, Nanotechnology, vol. 17, 2006, pp. 5954-5959.

[16] P. Royer, J.P. Goudonnet, R.J. Warmack and T.L. Ferell, “Substrate effects on surface-plasmon spectra in metal-island films”, Phys. Rev. B, vol. 35, 1987, pp.3753-3759.

[17] O.A. Yeshchenko, I.M. Dmitruk, A.A. Alexeenko and A.V. Kotko, “Surface Plasmon as a probe for melting of silver nanoparticles”, Nanotechnology, vol. 21, 2010, p. 045203 (6pp.).

[18] M. Khan et al., “Structural and thermal studies of silver nanoparticles and electrical transport study of their thin films”, Nanoscale Research Letters, vol. 6, 2011, p. 434 (8pp.), doi:10.1186/1556-276X-6-434.

[19] S.A. Little, T. Begou, R. E. Collins and S. Marsillac, “Optical detection of melting point depression for silver nanoparticles via in situ real time spectroscopic ellipsometry”, Appl. Phys. Lett., vol. 100, 2012, p. 051107 (4pp.).

[20] E.C. Garnett et al., “Self-limited plasmonic welding of silver nanowire junctions”, Nature Materials, vol.11, 2012, pp.241-249.

[21] G. Baffou, R. Quidant and C. Girard, “Heat generation in plasmonic nanostructures: Influence of morphology”, App. Phys. Lett., vol. 94, 2009, p. 153109 (3pp.).

[22] A. O. Govorov and H.H. Richardson, “Generating heat with metal nanoparticles”, Nanotoday, vol. 2, 2007, pp. 30- 38.

 ISBN: 978-1-61208-303-2